General Disclaimer

One or more of the Following Statements may affect this Document

- This document has been reproduced from the best copy furnished by the organizational source. It is being released in the interest of making available as much information as possible.

- This document may contain data, which exceeds the sheet parameters. It was furnished in this condition by the organizational source and is the best copy available.

- This document may contain tone-on-tone or color graphs, charts and/or pictures, which have been reproduced in black and white.

- This document is paginated as submitted by the original source.

- Portions of this document are not fully legible due to the historical nature of some of the material. However, it is the best reproduction available from the original submission.

NASA CR-132624

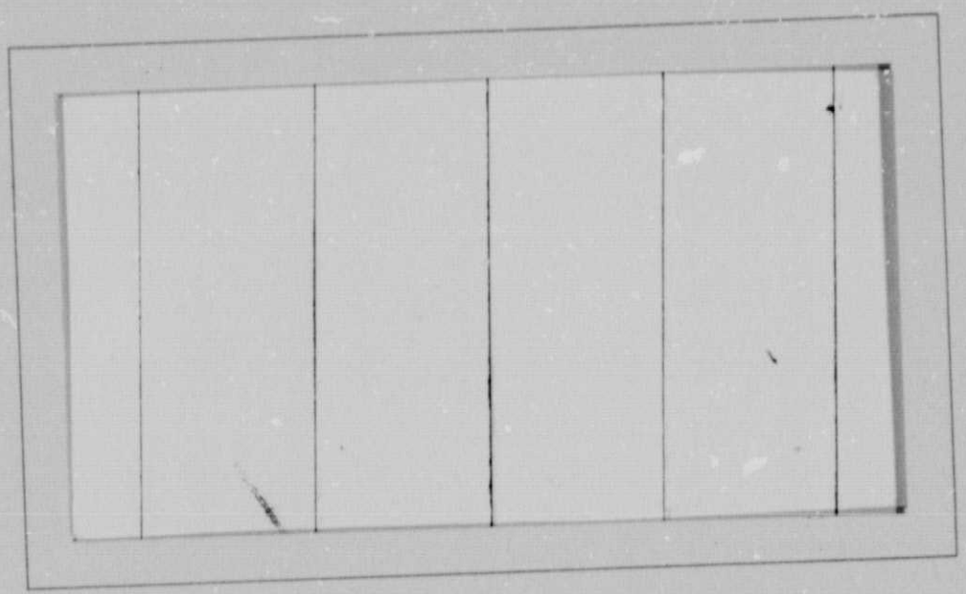

EARTH ENERGY EXPERIMENT (E^3) PROJECT

NASA CONTRACT NAS 1-11871

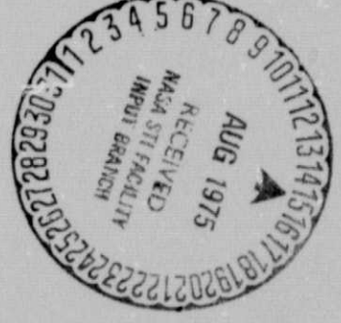

drexel university
PHILADELPHIA, PENNSYLVANIA 19104

DEPARTMENT OF PHYSICS
AND ATMOSPHERIC SCIENCE

NASA CR-132624

STEADY-STATE SOLUTION TO THE CONDUCTION PROBLEM OF A SPHERICAL BALLOON RADIOMETER

By Frederick B. House and
Alan J. Cimorelli

Final Report
Phases I and II

Prepared under Contract No. NAS1-11871 by
Department of Physics and Atmospheric Science
Drexel University
Philadelphia, Pennsylvania 19104

for

NATIONAL AERONAUTICS AND SPACE ADMINISTRATION

FOREWORD

The present report is part of broader effort which concerns an investigation of ESSA VII radiation data for use in long-term earth energy experiments, performed under Langley Research Center Contract No. NAS1-11871 for the National Aeronautics and Space Administration. This report is one of three companion reports which together constitute the final report of phases I and II of subject contract. The other two reports are entitled; "An Investigation of ESSA VII Radiation Data for Use in Long-Term Earth Energy Experiments," published as NASA CR-132623, and "Our Contaminated Atmosphere - The Danger of Climate Change," published as NASA CR-132625.

FOREWORD

The present report is part of broader effort which concerns an investigation of ESSA VII radiation data for use in long-term earth energy experiments, performed under Langley Research Center Contract No. NAS1-11871 for the National Aeronautics and Space Administration. This report is one of three companion reports which together constitute the final report of phases I and II of subject contract. The other two reports are entitled; "An Investigation of ESSA VII Radiation Data for Use in Long-Term Earth Energy Experiments," published as NASA CR-132623, and "Our Contaminated Atmosphere - The Danger of Climate Change," published as NASA CR-132625.

TABLE OF CONTENTS

LIST OF FIGURES

LIST OF TABLES

LIST OF SYMBOLS

Symbol	Definition	First Used Equation	First Used Page
T	Skin temperature of balloon radiometer, ^{o}K.	Text	2
σ	Stefan-Boltzmann constant $\sigma = 5.6697 \times 10^{-8}$ watts/m^2-K.	Text	2
a	Radius of balloon (see figure 1), m.	(1)	3
H_s	Irradiant sources absorbed by balloon - assumed parallel irradiation, watts/m^2.	(1)	3
W_e	External radiant power density from balloon area element - $W_e = \sigma T_e^4$, watts/m^2.	(1)	3
W_i	Internal radiant power density from balloon area element - $W_i = \sigma T_i^4$, watts/m^2.	(1)	3
T_e	Temperature of external area element of balloon skin, K.	(2)	5
T_i	Temperature of internal area element of balloon skin, K.	(3)	5
H_i	Irradiance on an internal area element from balloon's interior - $H_i = \sigma T_r^4$, watts/m^2.	(1)	3
T_r	Temperature of radiometer sensing internal irradiance H_i, K.	(1)	3
S	Surface area of balloon - $S = 4\pi a^2$, m^2.	(2)	5
$\overline{W}_e$	Average external radiant power density, watts/m^2.	(2)	5
$\overline{W}_i$	Average internal radiant power density, watts/m^2.	(3)	5
δ	Error parameter - $\delta \equiv 2(\overline{W}_e - \overline{W}_i)$, watts/$m^2$.	(5)	5
ϵ	Error in observing irradiant sources H_s, watts/m^2.	(6)	5
γ	Parameter defined as the ratio of skin thickness to average thermal conductivity, m^2/watt-K.	(10)	8
k	Coefficient of thermal conductivity, watt/(m-K).	Table 1	17
$\overline{k}$	Average coefficient of thermal conductivity for a balloon skin, watt/(m-K).	Table 2	18

STEADY-STATE SOLUTION TO THE CONDUCTION PROBLEM OF A SPHERICAL BALLOON RADIOMETER

INTRODUCTION

House and Sweet (1973) have proposed a satellite system for observing the earth's radiation balance employing spherical balloon radiometers. The instrumentation consists of three inflatable, spherical structures which are exposed to external irradiances of the radiation budget. In the steady-state condition of radiative equilibrium, the magnitudes of absorbed external irradiances are sensed by internal radiometers mounted on the skin of each balloon. The temperatures of the radiometers are monitored as a measure of the balloons' internal irradiances (equal to absorbed external irradiances) and then telemetered to earth. These temperatures will vary depending on the external optical properties of their respective balloons, whose properties are selected to effectively discriminate the components of the earth's radiation balance.

In the discussion of measurement principle cited above, two assumptions are made concerning conduction of heat:

- lateral conduction along the balloon skin represents a negligible contribution to the overall power density balance on an area element of a balloon.
- the difference between the inside and outside temperatures of an area element is negilgibly small.

The effect of lateral conduction becomes small when the balloon radius is many times larger than its thickness. In the case of the balloons considered above, the radius is about 10^4 times the thickness. Therefore, it is reasonable to neglect lateral heat conduction in the first approximation.

The assumption that the difference between the inside and outside temperatures of an area element is negligibly small implies that the skin is quite thin and/or the thermal conductivity is quite large. Materials under consideration will lead to balloon thicknesses from about 0.5 to 3.0 mils and possibly thicker for those surfaces which are painted. Thermal conductivities of materials will vary. In the case of aluminum it is large; however, plastics such as mylar and teflon, and paints have lower magnitudes of thermal conductivity. Small, but significant temperature gradients may be established across the skin for the balloon thicknesses and materials currently under consideration. Furthermore, the effect of temperature gradients through the skin are enhanced by the fourth power of temperature when considering radiant power densities according to Stefan-Boltzmann's Law σT^4.

The purpose of this investigation is to assess the conduction problem mathematically in order to determine its impact on measurement accuracy. It is desirable to develop the problem in terms of the magnitude of irradiant sources, balloon thickness and thermal conductivity so that the results may be utilized effectively in the engineering design of the satellite system under realistic irradiant environments.

PROBLEM DEVELOPMENT

Consider the measurement process depicted in figure 1. The spherical balloon shell absorbs radiant power from irradiant sources H_s over its cross-sectional area πa^2, assuming the upper limit case that all irradiation is parallel. When the balloon is in radiative equilibrium with its environment, the absorbed power is balanced by an equal loss of power W_e back to space from its surface area $4\pi a^2$. The magnitude of power loss from an area element depends on the external temperature T_e according to Stefan-Boltzmann's Law σT_e^4 if the balloon is a black body.

An internal radiometer is located at the inside skin of the balloon. This radiometer absorbs radiant power H_i from the inside of the balloon W_i where $W_i = \sigma T_i^4$. The temperature of this radiometer T_r is monitored and eventually telemetered to earth. The point in question is whether it is possible to work backwards from an observed temperature of the internal radiometer to obtain an accurate measurement of irradiant sources?

Several mathematical expressions hold for the balloon configuration under different bounding conduction assumptions. Under conditions of infinite conductivity, the balloon will be isothermal. Thus, $T_e=T_i=T_r$. Then,

$$\pi a^2 H_s = 4\pi a^2 W_e$$

and

$$\frac{1}{4} H_s = W_e = W_i = H_i = \sigma T_i^4 \qquad (1)$$

It is evident in equation (1) that H_s is related to the temperature observation T_r.

A more general case is to assume that lateral conduction can be neglected (i.e., the radius to thickness ratio is very large) and the skin thickness is quite small. For these conditions temperature gradients through the skin are negligible and $T_i = T_e$ for an area element.

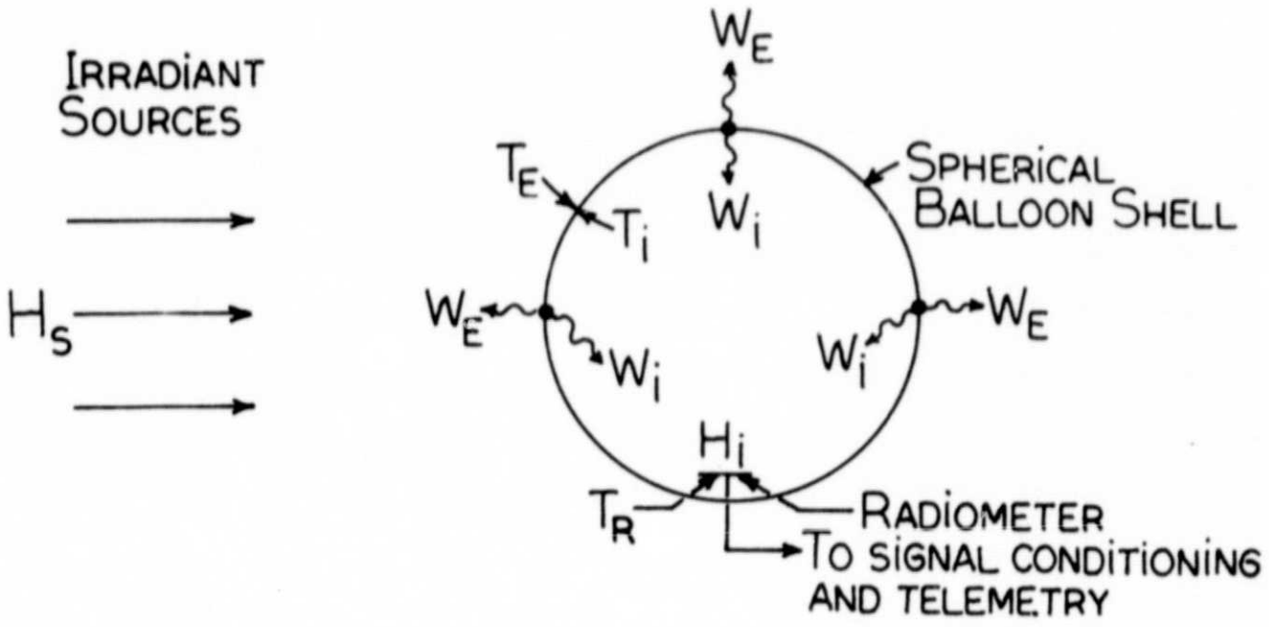

Figure 1. Schematic representation of measurement by a spherical balloon radiometer.

However, the temperature will vary from one area element to the other. Defining the external and internal average radiant power densities as

$$\overline{W_e} = \frac{1}{S}\int_S \sigma T_e^4 \, dS \tag{2}$$

and

$$\overline{W_i} = \frac{1}{S}\int_S \sigma T_i^4 \, dS \tag{3}$$

respectively, a similar chain relationship as equation (1) is valid:

$$\frac{1}{4} H_s = \overline{W_e} = \overline{W_i} = H_i = \sigma T_r^4 \tag{4}$$

Again the irradiant sources H_s are related to the observed temperature T_r.

The bounding conduction characteristics assumed in this work are:

- lateral conduction can be neglected
- conduction through the skin is a significant part of the heat transfer

When thermal conduction through the skin thickness is slow, $T_i \neq T_e$ and $H_i = \overline{W}_i \neq \overline{W}_e$ by some amount (see Figure 2a). This condition will lead to an error in measuring H_s, utilizing the observation T_r. Defining an error parameter $\delta = 2 (W_e - W_i)$, the error in the irradiant sources H_s, defined by ϵ, is related by

$$H_s = 4\overline{W_i} + \epsilon = 4\overline{W_i} + 2\delta = 4\overline{W_e} \tag{5}$$

where

$$\epsilon = 2\delta \tag{6}$$

The factor of two in equation (6) is for convenience in later mathematical development (see equation 9). The goal of the solution to the balloon conduction problem is to formulate the error ϵ in terms of the magnitude of irradiant sources H_s, the the thickness of the balloon and the thermal conductivity of balloon materials.

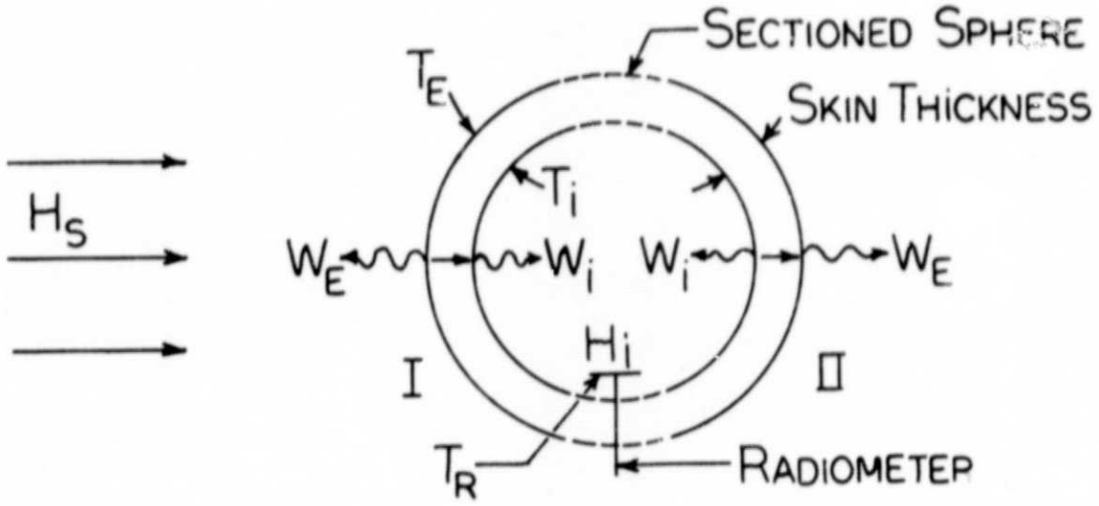

(2a)

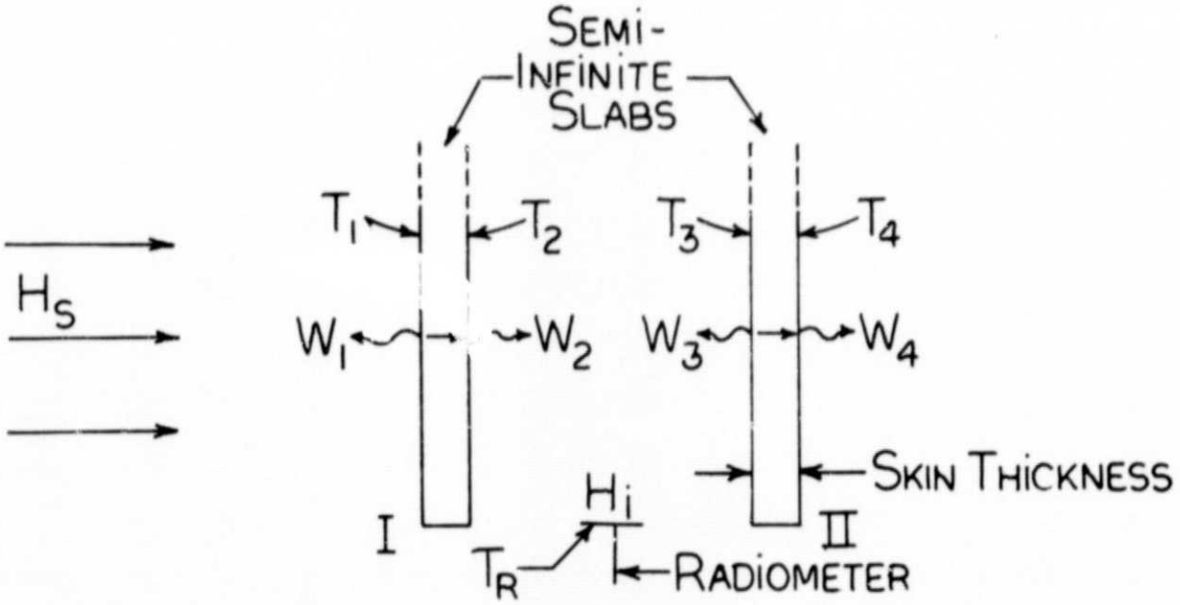

(2b)

Figure 2. Schematic representation of (a) balloon conduction problem and (b) approximation used in problem solution. Note: the irradiance on slab I is $\frac{1}{2} H_s$, providing the same average magnitude of irradiance per unit area as that on hemisphere I.

SOLUTION

The balloon conduction problem can be represented by the diagram in figure 2(a). In this case, the sphere is depicted as two separate hemispheres; one hemisphere (I) is exposed to irradiant sources H_s, and the second hemisphere (II) is in the shadow of the first. Since lateral conduction is negligible, the transfer of heat from the first to the second hemisphere is accomplished solely by radiative transfer within the balloon interior. The geometry in figure 2(a) is approximated nicely by considering each hemisphere as a semi-infinite slab of similar physical properties. This representation is shown in figure 2(b).

In the slab configuration, irradiation impinges on the outer surface of slab I. A portion of the radiant power is conducted through slab I, radiated to the inner surface of slab II, and, after conduction, exits from the outer surface of slab II. The radiometer views both slabs equally in figure 2(b) and in a manner similar to viewing both hemispheres in figure 2(a). Expressions relating various parameters discussed previously are as follows:

$$\overline{W_e} = \frac{W_1 + W_4}{2} = \frac{1}{4} H_s \tag{7}$$

$$\overline{W_i} = \frac{W_2 + W_3}{2} = H_i = \sigma T_i^4 \tag{8}$$

and

$$\delta = (W_1 + W_4) - (W_2 + W_3) \tag{9}$$

In figure 2(a), energy (heat) flows per unit area and time from the illuminated side, represented by temperature T_1, through slabs I and II, and is radiated out to space at an effective temperature T_4. For this energy flow to maintain itself, the relationship between temperatures is that $T_1 > T_2 > T_3 > T_4$.

A chain relationship depicting this energy flux (power) density is

$$\frac{1}{2}H_s - W_1 = \frac{1}{\gamma}(T_1 - T_2) = W_2 - W_3 = \frac{1}{\gamma}(T_3 - T_4) = W_4 \qquad (10)$$

where γ is the ratio of skin thickness to the thermal conductivity of the material in units of m/(watts/(m - K)). The expression $\frac{1}{\gamma}(T_1 - T_2)$ in equation (10), for example, is the power density conducted through slab I in units of watts/m^2. For simplicity the skin material is assumed to be homogeneous with an average thermal conductivity.

Referring again to figure 2(b), in the condition of radiative equilibrium, each of the four surfaces will be at temperatures T_j and corresponding radiant flux densities $W_j = \sigma T_j^4$. The thermal configuration of the system will depend only upon the magnitude of H_s, the plate thickness and the thermal conductivity of the materials. In this regard, four equations can be written using equation (10) to describe the steady-state condition of the system.

$$\frac{1}{2}H_s - W_1 = W_2 - W_3 \qquad (11a)$$

$$(T_1 - T_2) = \gamma\left(\frac{1}{2}H_s - W_1\right) \qquad (11b)$$

$$(T_3 - T_4) = \gamma(W_2 - W_3) \qquad (11c)$$

$$W_2 - W_3 = W_4 \qquad (11d)$$

Equations 11a and 11b describe the radiant power balance and the heat conduction, respectively, for slab I. Similarly, equations 11c and 11d describe conditions for slab II.

The problem at hand is now one of finding the simultaneous solution of the system of equations in set (11) with H_s and γ as adjustable parameters. Since these equations are non-linear in temperature, a simple algebraic solution is not possible. One way of approaching

this type of problem is to employ a perturbation technique involving a Jacobian operation which leads to an iterative solution to the equations. A further simplification results in the realization that it is not necessary to find a solution which explicitly determines all unknown quantities -- it is necessary only to find the parameter δ in equation (9).

The procedure for solution would be as follows:

1. Choose a γ such that the trivial solution (i.e., $\gamma=0$) for δ is found.
2. Perturb the initial choice to the general case (i.e., $\gamma > 0$).
3. Using the choice in 1. and the required perturbation as inputs to the Jacobian technique, find a solution for δ in terms of γ and H_s.

First assume that the material has an infinite conductivity (i.e., $\gamma = 0$). Then the equations in set (11) become

$$0 = g_{o1} = \frac{1}{2} H_s - W_1 - W_2 + W_3 \qquad (12a)$$

$$0 = g_{o2} = T_1 - T_2 \qquad (12b)$$

$$0 = g_{o3} = T_3 - T_4 \qquad (12c)$$

$$0 = g_{o4} = W_2 - W_3 - W_4 \qquad (12d)$$

Under this condition,

$$T_1 = T_2 \text{ implying that } W_1 = W_2 \qquad (13a)$$

$$T_3 = T_4 \text{ implying that } W_3 = W_4 \qquad (13b)$$

or, $W_1 + W_4 = W_2 + W_3$. Therefore,

$$\delta = (W_1 + W_4) - (W_2 + W_3) = 0$$

and no error in the measurement results.

Now perturb the solution above to the realistic case for $\gamma > 0$. In doing so equations in set (12) become

$$0 = g_1 = \tfrac{1}{2} H_5 - W_1 - W_2 + W_3 \tag{14a}$$

$$0 = g_2 = (T_1 - T_2) - \gamma\left(\tfrac{1}{2} H_5 - W_1\right) \tag{14b}$$

$$0 = g_3 = (T_3 - T_4) - \gamma\left(W_2 - W_3\right) \tag{14c}$$

$$0 = g_4 = W_2 - W_3 - W_4 \tag{14d}$$

The equations in set (14) have been changed by the following amounts

$$\Delta g_1 = \Delta g_4 = 0 = g_1 - g_{o1} = g_4 - g_{o4}$$

$$\Delta g_2 = -\gamma\left(\tfrac{1}{2} H_5 - W_1\right) = g_2 - g_{o2}$$

$$\Delta g_3 = -\gamma\left(W_2 - W_3\right) = g_3 - g_{o3}$$

where Δg_i, is defined as the required perturbation of the i^{th} equation.

Also for $\gamma > 0$ assume that

$$0 = (W_1 + \Delta W_1) + (W_4 + \Delta W_4) - (W_2 + \Delta W_2) - (W_3 + \Delta W_3) \tag{15}$$

Subtracting equation (15) from equation (9) gives

$$\delta = -\left[(\Delta W_1 + \Delta W_4) - (\Delta W_2 + \Delta W_3)\right] \tag{16}$$

where the ΔW_j's correspond to the changes in the power densities required to solve set (14). The ΔW_j's are found using the Jacobian technique.

The Jacobian operation on set (14) gives, in matrix form,

$$J(W)\,\Delta\vec{W} = \Delta\vec{g}$$

where $$(J(W))_{ij} = \partial g_i / \partial W_j$$

or

$$\begin{pmatrix} -1 & -1 & 1 & 0 \\ \gamma + 1/4\sigma T_1^3 & -1/4\sigma T_2^3 & 0 & 0 \\ 0 & -\gamma & \gamma + 1/4\sigma T_3^3 & -1/4\sigma T_4^3 \\ 0 & 1 & -1 & -1 \end{pmatrix} \begin{pmatrix} \Delta W_1 \\ \Delta W_2 \\ \Delta W_3 \\ \Delta W_4 \end{pmatrix} = \begin{pmatrix} 0 \\ -\gamma\left(\frac{1}{2} H_5 - W_1\right) \\ -\gamma\left(W_2 - W_3\right) \\ 0 \end{pmatrix} \tag{17}$$

Incorporating information in equation (10) and set (13), equation (17) can be expressed as four simultaneous equations

$$-\Delta W_1 - \Delta W_2 + \Delta W_3 = 0 \tag{18a}$$

$$(\gamma + 1/4\sigma T_1^3)\Delta W_1 - (1/4\sigma T_1^3)\Delta W_2 = -\gamma\left(\tfrac{1}{2}H_s - W_1\right) \tag{18b}$$

$$-\gamma\Delta W_2 + (\gamma + 1/4\sigma T_4^3)\Delta W_3 - (1/4\sigma T_4^3)\Delta W_4 = -\gamma(W_2 - W_3) \tag{18c}$$

$$\Delta W_2 - \Delta W_3 - \Delta W_4 = 0 \tag{18d}$$

If equations (18a) and (18d) are added,

$$-\Delta W_1 - \Delta W_4 = 0; \qquad \Delta W_1 = -\Delta W_4 \tag{19}$$

Therefore, the solution for δ in equation (16) reduces to

$$\delta = (\Delta W_2 + \Delta W_3) \tag{20}$$

The remaining portion of the problem involves the determination of $(\Delta W_2 + \Delta W_3)$ from equation set (18). However, the solution includes variables W_j and T_j in addition to H_s and γ. It is desirable to express the solution only in terms of the adjustable parameters H_s and γ. The following identities follow from equation (10) and set (13) which aid in the elimination of W_j and T_j.

$$H_s = 3W_1 \quad \text{AND} \quad T_1^3 = (H_s/3\sigma)^{3/4}$$

$$H_s = 6W_4 \quad \text{AND} \quad T_4^3 = (H_s/6\sigma)^{3/4}$$

The expression for the error parameter δ is

$$\delta = 0.0309\gamma H_s^{7/4}\left(\frac{6.57}{1.59\gamma H_s^{3/4} + 110.8}\right) \tag{21}$$

when a value of $\sigma = 5.6697 \times 10^{-8}$ watts/m^2-K^4 is used in the evaluation.

Equation (21) reduces to the compact expression

$$\delta = 0.0018\, \gamma\, H_s^{7/4} \tag{22}$$

since the $H_s^{3/4}$ term in the denominator is insignificant for reasonable values of $H_s < 2000$ watts/m^2 and $\gamma < 10^{-3}$ m^2-K/watt. From equation (6), the error in the observed irradiant sources becomes

$$\epsilon = 0.0036\, \gamma\, H_s^{7/4} \tag{23}$$

Equation (23) can also be expressed as a percent error of H_s.

$$\text{ERROR} = \frac{\epsilon}{H_s} \times 100 = 0.36\, \gamma\, H_s^{3/4}\ (\%) \tag{24}$$

This concludes the development of a steady-state solution to the conduction problem of a spherical balloon radiometer. The impact of these observational errors as related to earth radiation balance measurements are discussed in the results section below.

RESULTS

The solution to the conduction problem in equation (23) indicates, as would be expected from the physical characteristics of the problem, that the observational error of a balloon radiometer increases as the magnitude of irradiant sources increases, as the balloon thickness increases and as the thermal conductivity of the skin materials decreases. Quantitatively ϵ increases as the 1.75 power of H_s and is directly proportional to the parameter γ. Thus, the observational error increases linearly with balloon thickness and inversely with the thermal conductivity of the materials. Consequently, skin materials such as aluminum which are good thermal conductors have reduced observational errors, whereas, plastics which are poor thermal conductors have larger observational errors compared to aluminum. Also the solution indicates that thin skinned balloons are a desirable engineering design goal.

Further examination of equation (23) indicates that the errors in observations comprise a family of straight, parallel lines on a log-log plot of ϵ vs. γ, having slopes of one. Figure 3 presents such a plot for representative values of H_s and γ. In order to utilize figure 3, all one has to do is compute the ratio of skin thickness to average thermal conductivity, and then examine the variation in the observational error for different magnitudes of irradiant sources associated with components of the earth radiation balance. As an example, assume the parameter $\gamma = 5 \times 10^{-4}$ in magnitude, the observational error during typical nighttime observations (H_s = 240 watts/m^2) would be .026 watts/m^2, and during daytime observations (H_s = 1800 watts/m^2) is .90 watts/m^2.

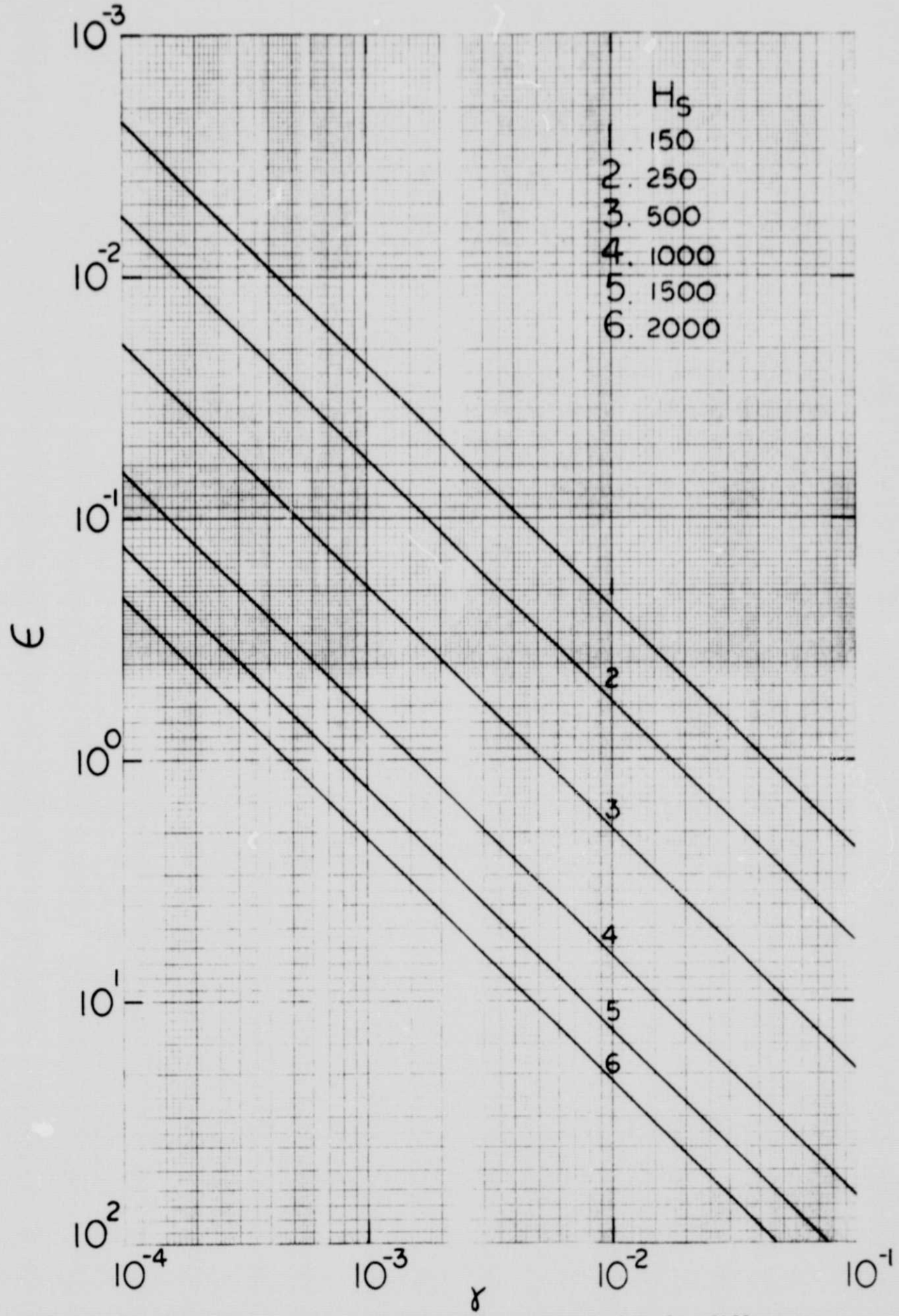

Figure 3. Variation in the observational error ϵ with γ for different magnitudes of irradiant sources H_s, watt/m^2.

In a similar manner, equation (24) can be plotted on a log-log graph of % error vs. γ. The graph in figure 4 illustrates such a plot for representative values of H_s. This graph can be utilized in the same manner as that in figure 3. The percentage errors associated with the examples above for nighttime and daytime observations are .01% and .05%, respectively.

The balloon radiometers discussed by House and Sweet (1973) consist of thin, laminated layers of aluminum and plastic materials which are joined by an adhesive. Three balloons are employed in their satellite system having different external optical properties. One balloon is painted black, the second is white (either a paint or second surface mirror) and the third is an aluminum surface. These balloons may be denoted by the optical colors as black, white and aluminum.

Estimates of the observational errors caused by thermal conduction through the balloon skin were made, using the solution developed in this work. The thermal properties and construction characteristics are needed in order to determine these errors. Table I is a list of thermal conductivities for paints and various balloon materials. Table 2 summarizes the construction details of realistic balloons under consideration. Weighted average thermal conductivities were computed from the coefficients in Table 1, weighted by the thickness of each material. Aluminum is neglected in the calculations since the conductivity is large compared to other materials and, therefore, contributes little to the observational error. Corresponding magnitudes of γ were computed for each of the balloon configurations in Table 2.

It should be borne in mind when using the graphs in figures 3 and

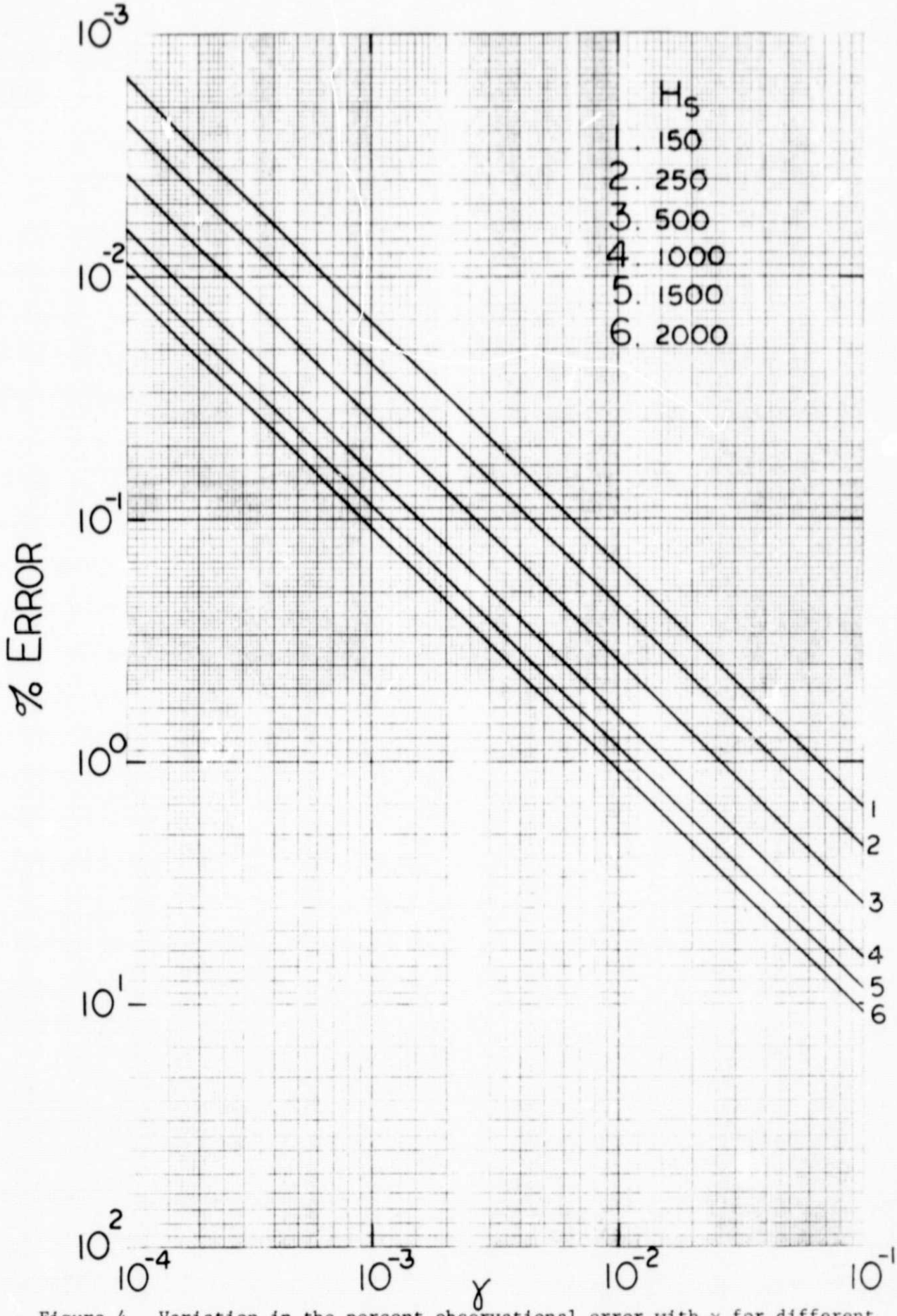

Figure 4. Variation in the percent observational error with γ for different magnitudes of irradiant sources H_s, watt/m^2.

TABLE 1

Approximate Thermal Conductivities of Balloon Materials

Material	Coefficient of Thermal Conductivity k, watt/(m-K)
Black paint	0.17
White paint	0.17
Aluminum	221.0
Mylar	0.15
Teflon	0.21
Adhesive	0.20
Captone	0.20

TABLE 2

Thickness of Construction Materials and Conductivity

Parameters of Typical Balloon Radiometers

External Balloon Color	Material	Thickness d, mil	Average Conductivity $\bar{k}$, (watt/(m-K))	Parameter γ, $((m^2-K)/watt)$
Aluminum	Aluminum*	0.5	0.17	1.4×10^{-4}
	Captone	0.2		
	Adhesive	0.2		
	Mylar	0.5		
Black	Black Paint	3.0	0.17	5.5×10^{-4}
	Aluminum*	0.5		
	Adhesive	0.2		
	Mylar	0.5		
White Painted	White Paint	5.0	0.19	7.6×10^{-4}
	Aluminum*	0.5		
	Adhesive	0.2		
	Mylar	0.5		
White Anodized Al	Aluminum*	2.0	0.16	1.1×10^{-4}
	Adhesive	0.2		
	Mylar	0.5		
White 2d Surface Mirror using Teflon.	Teflon	2.0	0.20	3.4×10^{-4}
	Aluminum*	0.5		
	Adhesive	0.2		
	Mylar	0.5		

*
Aluminum is neglected in the calculations because of its large coefficient of thermal conductivity.

4 that the theory developed herein applies to a perfectly black balloon. The balloons listed in Table 2 have varying optical properties both externally and internally. The black balloon most closely approaches the idealized situation of the solution to the conduction problem in equation (23). The white balloons will absorb about one fourth as much direct and reflected solar radiation as the black balloon. However, the thermal emitting properties of the white balloons would be similar to that of a black balloon.

The aluminum balloon is considerably different than either the white or black balloons. An aluminum surface absorbs about the same portion of solar radiation as the white balloon. But the capacity of an aluminum surface to loose heat through thermal emission is about five percent that of a black balloon.

Surfaces exposed to solar radiation frequently are classified by their external shortwave absorptivity to longwave emissivity ratio, termed the alpha over epsilon ratio. For the surfaces under consideration, the black balloon has an optical ratio of about 1.0, the white balloon about 0.25 and the aluminum balloon about 4.0 in magnitude. As a result, the white balloon acquires an equilibrium temperature colder than the black balloon, and the aluminum balloon is warmer than the black balloon.

One approach in the application of the theory to a balloon with typical optical properties is to scale the incident irradiance H_s by the corresponding alpha over epsilon ratio. Using the above ratio magnitudes, a value of irradiance H_s equal to 1600 watts/m^2 for the black balloon would be increased to 6400 watts/m^2 for the aluminum balloon and reduced to 400 watts/m^2 for the white balloon. This approach is a first order approximation which can be justified for purposes of this preliminary analysis.

Observational errors for the balloon configurations of figure 2 are summarized in figure 3. Night and day values of 240 and 1800 watt/m^2 were assumed, respectively, as reasonable magnitudes of irradiance H_s (see black balloon in table 3). These magnitudes are scaled by the alpha over epsilon ratios above and are listed in table 3, for reference. Observational errors for the black and aluminum balloons are larger than those for the white balloon even though the parameter in table 2 for the white balloon is larger than that for the other two balloons. During daytime observations, the error magnitude for the white balloon is 0.12 watt/m^2, whereas, the errors for the black and aluminum balloons may be as much as 0.98 watt/m^2 and 2.84 watt/m^2, respectively. In terms of percent errors of H_s, all values are less than 0.05 percent.

It should be kept in mind when analyzing the results that the assumption is made where the incident irradiances all come from the same direction. Such an assumption maximizes the observational error. In reality, a balloon radiometer in orbit is exposed to irradiances from various directions and of different magnitudes, depending on the relative positions of the satellite, earth and sun. When these irradiances are incident on different portions of the balloon skin, the observational error is reduced since the surface area of the balloon is at a more uniform temperature. Thus, the estimates of observational errors in table 3 are larger than would be expected under normal operating conditions in orbit.

In summary, the results of this analysis indicate that observational errors during the day are at least an order of magnitude larger during daytime observations than those at night. Observations by all three white balloon configurations are acceptable both during daytime and nighttime

TABLE 3

Estimated Observational Errors of

Typical Balloon Radiometers

Balloon Color	Scaled Irradiances H_s, watt/m^2	Observational Error ϵ, watt/m^2	Observational Error in (%)
Black	Night - 240	0.03	0.01
	Day - 1800	0.98	0.05
Aluminum	Night - 960	0.08	0.01
	Day - 7200	2.84	0.04
White Painted	Night - 60	0.003	0.01
	Day - 450	0.01	0.03
White Anodized Aluminum	Night - 60	0.001	0.001
	Day - 450	0.02	0.004
White 2d Surface Mirror Teflon	Night - 60	0.002	0.003
	Day - 450	0.05	0.01

modes of operation. In the case of the black balloon, observational errors are less than 1.0 watt/m^2 during the day and probably about 0.5 watt/m^2 for realistic orbital conditions. These errors are acceptable for purposes of earth energy budget observations.

Finally, errors for the aluminum balloon are less than 0.1 watt/m^2 at night, but may be as large as 2.8 watt/m^2 during daytime operation. The latter magnitude may not be acceptable for accurate observations of the earth energy budget. However, it should be remembered that the solution to the conduction problem developed in this report applies to black optical properties, considerably different than an aluminum surface. The results here suggest that a more detailed model of the conduction problem should be developed to determine a better estimate of the observational error for an aluminum balloon radiometer.

REFERENCES

House, F.B., Sweet, G.E. et al, 1973: Long-term Zonal Earth Energy Budget Experiment (LZEEBE). A proposal submitted to AAFE, NASA Langley Research Center, Hampton, Va.